Translational Oncology 42 (2024) 101891

Contents lists available at ScienceDirect

Translational Oncology

journal homepage: www.elsevier.com/locate/tranon

Original Research

Distinct leukocyte populations and cytokine secretion profiles define tumoral and peritumoral areas in renal cell carcinoma

Martina Borcinova [a], Robin Bartolini [b], Lily Koumbas Foley [c], Vojtech Novak [d], Pavla Taborska [e], Dmitry Stakheev [e], Michal Rataj [e], Daniel Smrz [e], Martina Fialova [f], Jaromir Hacek [g], Martin Komarc [h], Stepan Vesely [d], Marek Babjuk [d], Ilja Striz [f], Jirina Bartunkova [e], Tomas Buchler [i], Zuzana Ozaniak Strizova [e,*]

[a] Gynecologic Oncology Centre, First Faculty of Medicine, Charles University and General University Hospital in Prague, Czech Republic
[b] Lausanne Center for Immuno-oncology Toxicities (LCIT), Service of Immunology and Allergy, Department of Medicine, Lausanne University Hospital, University of Lausanne, Lausanne, Switzerland
[c] Chemokine Research Group, Institute of Infection, Immunity and Inflammation, College of Medical, Veterinary and Life Sciences, University of Glasgow, Glasgow G12 8TT, UK
[d] Department of Urology, Second Faculty of Medicine, Charles University and University Hospital Motol, Prague, Czech Republic
[e] Department of Immunology, Second Faculty of Medicine, Charles University and University Hospital Motol, Prague, Czech Republic
[f] Department of Immunology, Institute for Clinical and Experimental Medicine, Prague, Czech Republic
[g] Department of Pathology and Molecular Medicine, Second Faculty of Medicine, Charles University, Prague, Czech Republic
[h] Department of Methodology, Faculty of Physical Education and Sport, Charles University, Prague, Czech Republic
[i] Department of Oncology, Second Faculty of Medicine, Charles University and University Hospital Motol, Prague, Czech Republic

ARTICLE INFO

Keywords:
Kidney cancer
Tumor-infiltrating lymphocytes
Tumor immune microenvironment
Renal carcinoma immunotherapy
RCC TME
CAFs
CD8 T cells
peritumoral tissue
kidney cancer cytokines
cytotoxicity
PECAM-1

ABSTRACT

Renal cell carcinoma (RCC) is a common malignancy frequently diagnosed at the metastatic stage. We performed a comprehensive analysis of the tumor immune microenvironment (TIME) in RCC patients, including the peritumoral tissue microenvironment, to characterize the phenotypic patterns and functional characteristics of infiltrating immune cells. T cells from various compartments (peripheral blood, tumor, peritumoral area, and adjacent healthy renal tissue) were assessed using flow cytometry and Luminex analyses, both before and after T cell-specific stimulation, to evaluate activation status and migratory potential. Our findings demonstrated that tumor-infiltrating lymphocytes (TILs) exhibited heightened cytokine production compared to peritumoral T cells (pTILs), acting as the primary source of cytotoxic markers (IFN-γ, granzyme B, and FasL). $CD8^+$ T cells primarily employed Fas Ligand for cytotoxicity, while $CD4^+$ T cells relied on CD107a. In addition, a statistically significant negative correlation between patient mortality and the presence of $CD4^+CD107^+$ pTILs was demonstrated. The engagement with the PD-1/PD-L1 pathway was also more evident in $CD4^+$ and $CD8^+$ pTILs as opposed to TILs. PD-L1 expression in the non-leukocyte fraction of the tumor tissue was relatively lower than in their leukocytic counterparts and upon stimulation, peripheral blood T cells displayed much stronger responses to stimulation than TILs and pTILs. Our results suggest that tumor and peritumoral T cells exhibit limited responsiveness to additional activation signals, while peripheral T cells retain their capacity to respond to stimulatory signals

Abbreviations: RCC, Renal cell carcinoma; ccRCC, Clear cell renal cell carcinoma; non-ccRCCs, Non-clear cell renal cell carcinomas; ICIs, Immune checkpoint inhibitors; PD-1, Programmed cell death 1; PD-L1, Programmed cell death ligand 1; CTLA-4, Cytotoxic T-lymphocyte antigen 4; TKIs, Tyrosine kinase inhibitors; TME, Tumor microenvironment; TILs, Tumor-infiltrating lymphocytes; pTILs, Peritumoral tissue-infiltrating lymphocytes; CAFs, Cancer-associated fibroblasts; PBMCs, Peripheral blood mononuclear cells; FACS, Fluorescence-activated cell sorting; Luminex, Luminex assay; FN-γ, Interferon gamma; TRAIL, Tumor-necrosis factor-related apoptosis-inducing ligand; FasL, Fas Ligand; CXCL, Chemokine (C-X-C motif) ligand; PECAM-1, Platelet endothelial cell adhesion molecule-1; CD8+, Cluster of Differentiation 8 positive T cells; CD4+, Cluster of Differentiation 4 positive T cells; TGF-β, Transforming Growth Factor beta; TNF-α, Tumor Necrosis Factor-alpha; CD107a, Cluster of Differentiation 107a; CXCL-10, C-X-C motif chemokine ligand 10; CXCL-9, C-X-C motif chemokine ligand 9; CAFs, Cancer-Associated Fibroblasts.

* Corresponding author: Department of Immunology, Second Faculty of Medicine, Charles University and University Hospital Motol, V Uvalu 84, 150 06 Praha 5, Czech Republic.

E-mail address: zuzana.strizova@fnmotol.cz (Z. Ozaniak Strizova).

https://doi.org/10.1016/j.tranon.2024.101891
Received 11 July 2023; Received in revised form 17 November 2023; Accepted 23 January 2024

Introduction

Kidney cancer, one of the most common cancers in humans, is a therapeutically challenging malignancy [1]. The most prevalent subtype is clear cell renal cell carcinoma (ccRCC), while the remaining types are collectively known as non-clear cell RCCs (non-ccRCCs), displaying genetic and histological heterogeneity [2]. Upon diagnosis, approximately 30 % of the patients present with metastatic lesions [3,4]. Although targeted therapies have advanced, their efficacy in terms of overall survival diminishes once their effectiveness wanes [3].

In 2015, the anti-programmed cell death 1 (PD-1) monoclonal antibody nivolumab was approved for the treatment of patients with metastatic RCC. Since then, other immune checkpoint inhibitors (ICIs), including pembrolizumab, avelumab, and ipilimumab, targeting PD-1, programmed cell death ligand 1 (PD-L1), and cytotoxic T-lymphocyte antigen 4 (CTLA-4), respectively, have been implemented into routine clinical practice [5–7].

These agents, particularly when combined with other ICIs or tyrosine kinase inhibitors (TKIs), have radically improved the outcomes of systemic therapy for patients with RCC [6–9].

Hence, some patients still fail to respond to ICIs, and unconventional responses, such as pseudoprogression or tumor flares, have been observed [10–12]. Factors contributing to positive treatment responses include immune checkpoint molecule expression, high neoantigen load, and infiltration of CD8+ T cells. Therefore, a thorough analysis of the tumor microenvironment (TME) is crucial [13].

Peritumoral lymphocytes have emerged as important prognostic markers in various cancers [14–19], yet their precise role in the tumor-immune system interplay remains unclear. Understanding the microenvironment, immune cell phenotypes, and functions in the tumor and peritumoral regions may facilitate personalized treatments [20,21].

Our study fills a gap by investigating the phenotypic patterns and functional abilities of peritumoral lymphocytes in RCC. We comprehensively analyzed the tumor microenvironment, immune cell characteristics, and cytokine profiles to gain insights into their functional capacities.

Materials and methods

Human samples

Fresh human tissue samples (n = 68) were obtained from patients with RCC after nephrectomy (n = 20). Table 1 summarizes the cohort's baseline characteristics, with a majority having clear cell carcinoma (n = 17) and a subset exhibiting non-clear cell carcinoma (n = 3/papillary2x/collecting duct1x).

Table 1
Baseline Characteristics of the Study Cohort Demographic information detailing patients and characteristics of their respective tumors.

Characteristic	Patients (n)	Patients (%)
Age		
> 75	5	25.0
75 – 65	8	40.0
< 65	7	35.0
Sex		
Male	11	55.0
Female	9	45.0
Histology		
Clear cell RCC	17	85.0
Non-clear cell RCC	3	15.0
Tumor grade		
1	2	10.0
2	11	55.0
3	4	20.0
4	2	10.0
Not available	1	5.0
TNM tumor stage		
T1	14	70.0
T2	0	0
T3	4	20.0
Not available	2	10.0

Tissue samples included tumors, peritumoral tissue, adjacent healthy renal tissue, and peripheral blood. Peritumoral tissue was excised 1 cm from the tumor edge, and healthy renal tissue was collected farthest from the tumor edge. Samples were transferred into the laboratory in saline solution. Peripheral blood from two healthy donors was used as a control in specific subanalyses. The study adhered to the Declaration of Helsinki, with patient's written consent and approval from the Ethics Committee (No.EK-377/13). Cytokine analysis was conducted on 28 samples using Luminex and 38 samples using flow cytometry. The study design is illustrated in Fig. 1, outlining sample collection and selected analyses.

Cell isolation

Peripheral blood mononuclear cells (PBMCs) were isolated from 9 ml of whole blood using Isopaque-Ficoll. Leukocytes from tumors, peritumoral tissue, and healthy renal tissue were isolated as described previously [16]. Tissue samples were mechanically dissociated, incubated with RPMI-1640 medium supplemented with collagenase and DNAse, and filtered through a 70-µm strainer. Flow cytometry analyzed 40 cell suspensions from tumors, peritumoral tissue, healthy renal tissue, and PBMCs. In total, 28 cell suspensions from various tissues, including PBMCs, were stimulated with anti-CD3:CD28 beads after 24-hour incubation in RPMI 1640 medium.

Flow cytometry

Multicolor flow cytometry was used to characterize the phenotypic patterns of the tumor-infiltrating lymphocytes (TILs), peritumoral tissue-infiltrating lymphocytes (pTILs), and cancer-associated fibroblasts (CAFs) *ex vivo*. The isolated cells were stained with fluorophore-conjugated protein-specific antibodies (anti-CD45, clone MEM28, cat. n. 537,962, Exbio; anti-CD4, clone MEM421, cat.n.538380, Exbio; anti-CD8, clone MEM31, cat.n.531603, Exbio; anti-CD31,clone WM59,cat.n. B276836, Biolegend; anti-CD107a, clone H4A3, cat.n.529783; anti-PD-L1, clone 29E.2A3, cat.n.329734, Exbio; anti-CD95, cat.n. 305,611, Exbio; anti-CD178, clone NOK-1,cat.n.B321945,Biolegend; anti-hFAP, cat.n. AEHH221, RD Systems; anti-hαSMA, cat.n. ACAK0318071,RD Systems, anti-CD261, cat.n. 307,206, Biolegend)for 30 min, washed, and analyzed using a BD LSRFortessa flow cytometer (Becton Dickinson). The obtained data were analyzed using the FlowJo software (Tree Star, Ashland, OR, USA, version 10.6.1).

Selective T-cell stimulation

T cells ($CD4^+$ and $CD8^+$) isolated from the tissue samples/PBMCs were activated by superparamagnetic polymer beads with an optimized mixture of anti-CD3 and anti-CD28 monoclonal antibodies (Dynabeads Human T-Activator CD3/CD28, Gibco, Thermo Fisher Scientific). The assay was performed in accordance with the manufacturer's instructions. $CD3^+$ *T* cells were stimulated with anti–CD3/CD28 beads for 24 h. After stimulation, the suspensions were centrifuged, and the supernatant was analyzed using the Luminex cytokine assay.

Luminex cytokine assay

Supernatants from 28 cell suspensions were analyzed for interferon gamma (IFNγ), tumor-necrosis factor related apoptosis-inducing ligand (TRAIL), Fas Ligand (FasL), granzyme B, chemokine (C-X-C motif) ligand (CXCL)−9, CXCL-10, and platelet endothelial cell adhesion molecule-1 (PECAM-1) using the Luminex cytokine assay. A customized Luminex Human Magnetic Assay (Biotechne, R&D Systems s.r.o.,

Prague) was used to detect selected cytokines/chemokines in cell suspensions from four distinct compartments. Samples were acquired using the Bio-Plex 200 system.

Data analysis

Statistical analyses used SPSS (version 25.0) and GraphPad Prism 6. Correlation matrices were plotted using Corrplot (R package). Data presented as mean ± SEM, unless specified. Spearman's rank-order correlation coefficient assessed bivariate associations. Mann-Whitney U and Wilcoxon tests used Monte Carlo resampling ($N = 10{,}000$ samples), compensating for tied values. $\alpha = 0.05$ (P values: $^{*}P<0.05$, $^{**}P<0.01$, $^{***}P<0.001$, $^{****}P<0.0001$).

Results

Low CAF proportion is associated with higher PECAM-1 expression

First, we aimed to characterize the cellular populations in the peritumoral and tumoral areas of RCC samples, with a focus on cancer-associated fibroblasts (CAFs) and T-cells, which are key mediators of antitumor function.

CAFs have diverse functions in the tumor microenvironment (TME), with the ability to either promote or hinder tumor growth, as they interact with both tumor cells and tumor-infiltrating immune cells (TIICs) [22,23]. CAF-secreted factors have been shown to suppress T cell infiltration, proliferation, and cytotoxicity, while promoting Treg recruitment and differentiation [16,23,24]. CAF-induced increase in extracellular matrix density can also exclude T cells from the tumor area [25]. In our study, CAFs were defined as $CD45^{-}aSMA^{+}FAP^{+}$ cells [26,27]. We found that T cell proportions were similar across the tested tissue compartments, but CAFs, although representing only a minor fraction of viable CD45-negative cells varied between these compartments (Fig. 2a). Despite being the most abundant stromal cell population in many tumors, CAFs represented a small fraction in RCC samples, with higher relative abundance in the peritumoral area (3.9 % ±3.6 %) compared to the tumor area (0.8 % ±1.2 %), (Fig. 2b). The proportion of CAFs did not correlate with patient age, sex, tumor histology, grade, or stage. However, CAFs showed a significant negative correlation with $PECAM\text{-}1^{+}CD8^{+}$ T cells, which are critical for T cell transendothelial migration (Fig. 2c). It has been already shown that CAFs modulate T cell migration by altering the TME composition and thus, inhibit $CD8^{+}$ T cell trafficking and recruitment [16,23]. It is important to note that CAFs constituted only a minor fraction of viable cells, necessitating further research to fully understand the implications of these findings.

PECAM-1 expression is higher in $CD8^{+}$ T cells than in $CD4^{+}$ T cells

The PECAM-1-mediated interactions between migrating T cells and the endothelium facilitate and coordinate T cell extravasation (Fig. 3a). PECAM-1 expression also enhances transforming growth factor beta (TGF-β)-mediated inhibition of T cells, reducing their activation and secretion of IFN-gamma (IFN-γ) and tumor necrosis factor-alpha (TNFα) [28],. In addition, engagement of PECAM-1 enhances the anti-inflammatory properties of $CD8^{+}$ T cells, prevents apoptosis, and reduces T cell receptor signaling in $CD4^{+}$ T cells [29].

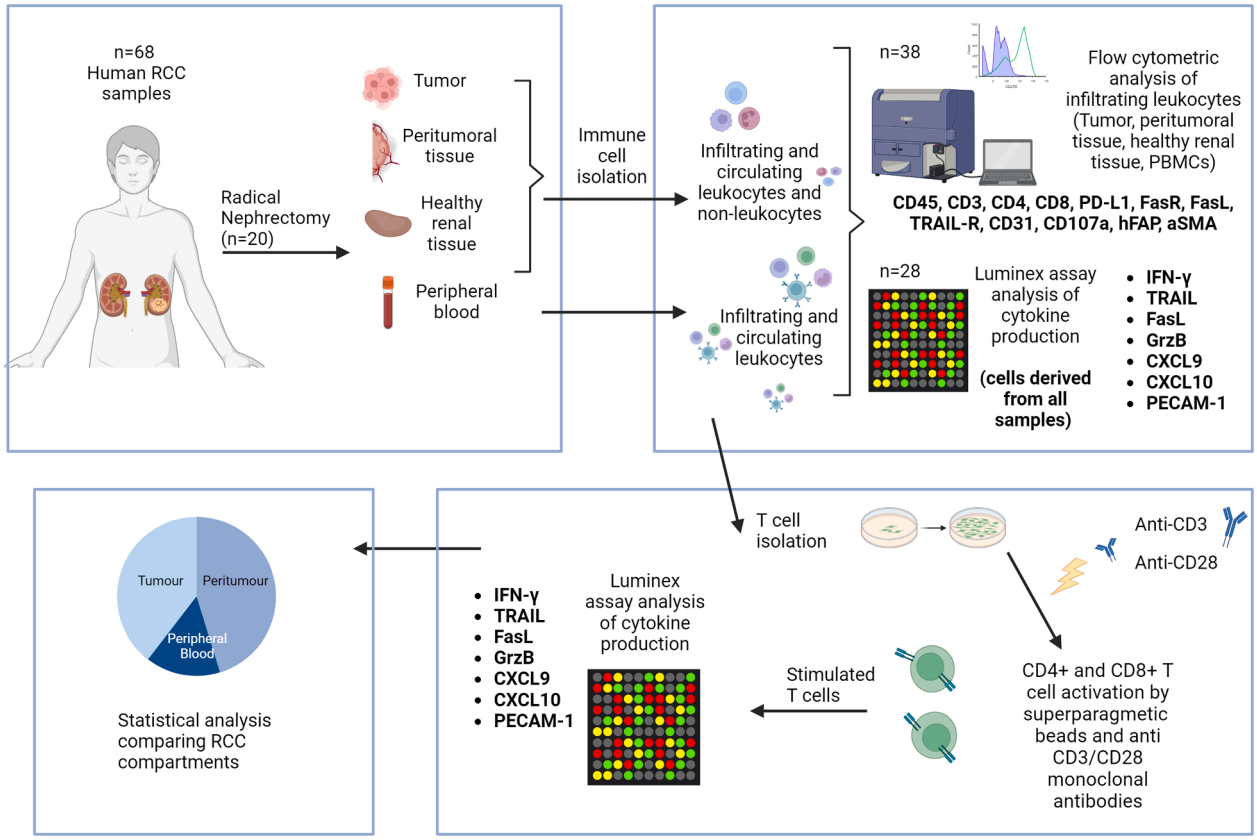

Fig. 1. Study design. A comprehensive representation of the study design. In the upper left corner, the figure illustrates the process of sample collection, encompassing the acquisition of biological specimens from the study participants. In the upper right corner, subsequent analyses of immune cells, involving techniques such as flow cytometry (FACS) and luminex assays, are depicted. The lower right section of the figure portrays the specific T cell stimulation procedure employed, along with the selected markers utilized for the analysis of T cell activation status. Finally, the lower left section demonstrates the statistical comparison phase, where appropriate statistical tests are performed to evaluate the significance of the obtained results. Created with Biorender (Ref.No. UR25FT8MNJ). IFNg: interferon gamma, TRAIL: TNF-related apoptosis-inducing ligand; FasL: Fas ligand; GrzB: Granzyme B; PECAM-1: Platelet Endothelial Cell Adhesion Molecule-1.

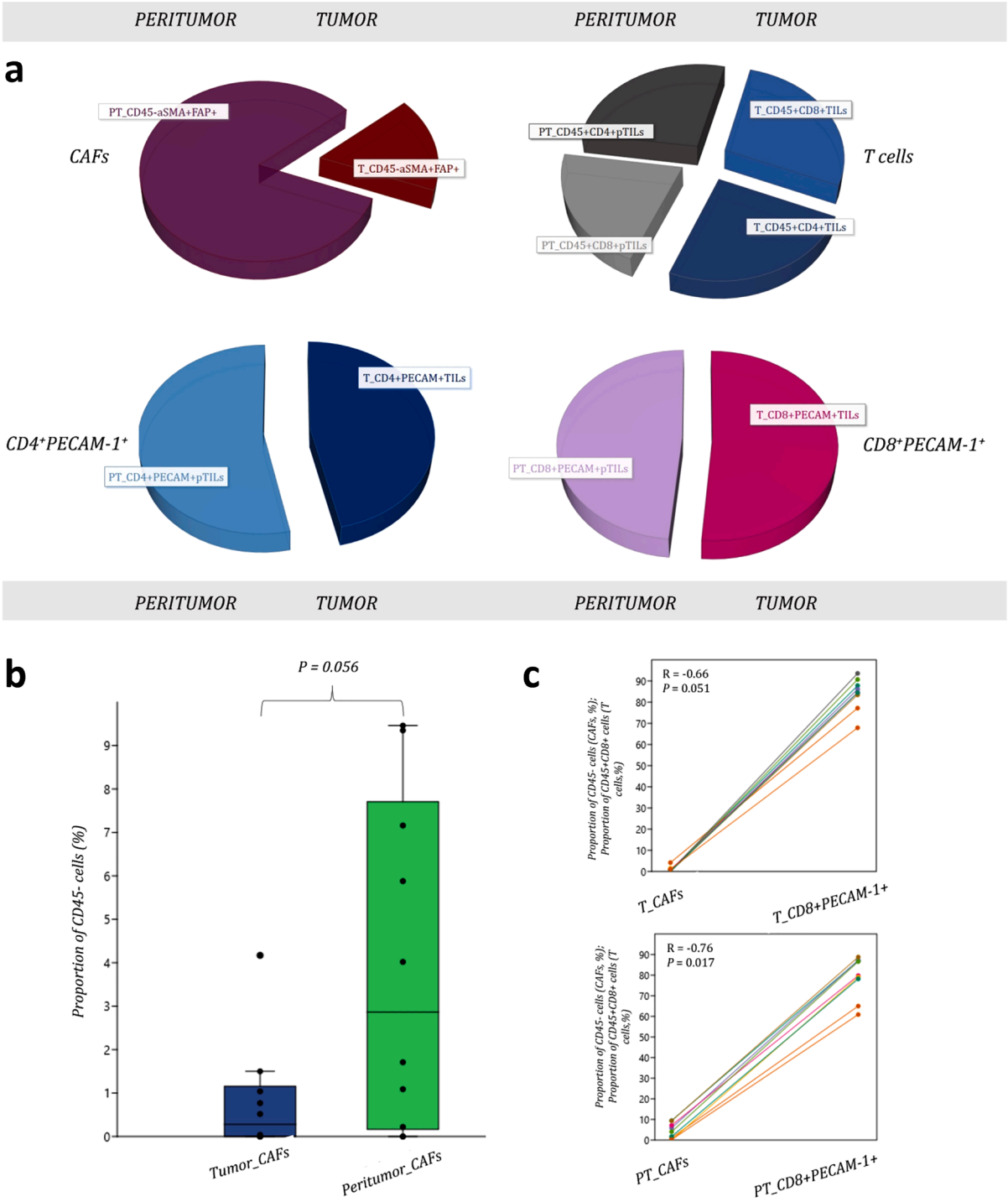

Fig. 2. Correlation of cancer-associated fibroblasts (CAFs) and PECAM-1 expression by $CD8^+$ T cells. A: four pie charts illustrating variations in the mean cellular ratios between the tumor and the peritumoral area. B: boxplots of relative abundance of CAFs in the tumoral and peritumoral compartments. The percentile range was set at 25 %, 50 %, and 75 %. The whisker range was chosen to be between minimal and maximal measured values with outliners. C: correlation between CAFs and $CD8^+PECAM\text{-}1^+$ producing cells in tumoral and peritumoral compartments. CAFs: cancer-associated fibroblasts; peritum: peritumoral tissue.

Based on the profound effects of PECAM-1 on T cell function, we examined its levels in $CD4^+$ and $CD8^+$ TILs and pTILs. Although PECAM-1 expression was comparable in the two tissue compartments, it was significantly higher in $CD8^+$ T cells than in $CD4^+$ T cells (Fig. 3b).

In the tumor and peritumoral tissue, the mean proportions of $PECAM\text{-}1^+CD8^+$ T cells were 84.0 % (±7.2 %) and 79.2 % (±9.5 %), respectively, while those of $PECAM\text{-}1^+CD4^+$ T cells were 26.8 % (±8.8 %) and 19.0 % (±15.3 %), respectively. PECAM-1 expression showed no association with the patient's age, sex, tumor stage, and grade **(Supplementary Figure 1).**

$CD8^+$ and $CD4^+$ T cell cytotoxicity is mediated by FAS ligand and CD107a, respectively, in RCC

To evaluate cytotoxic capacities in RCC tumors, we assessed tumoricidal mechanisms of $CD4^+$ and $CD8^+$ T cells infiltrating tumoral and peritumoral tissues, considering the impact of PECAM-1 expression on T cell subsets, activation state, and TME.

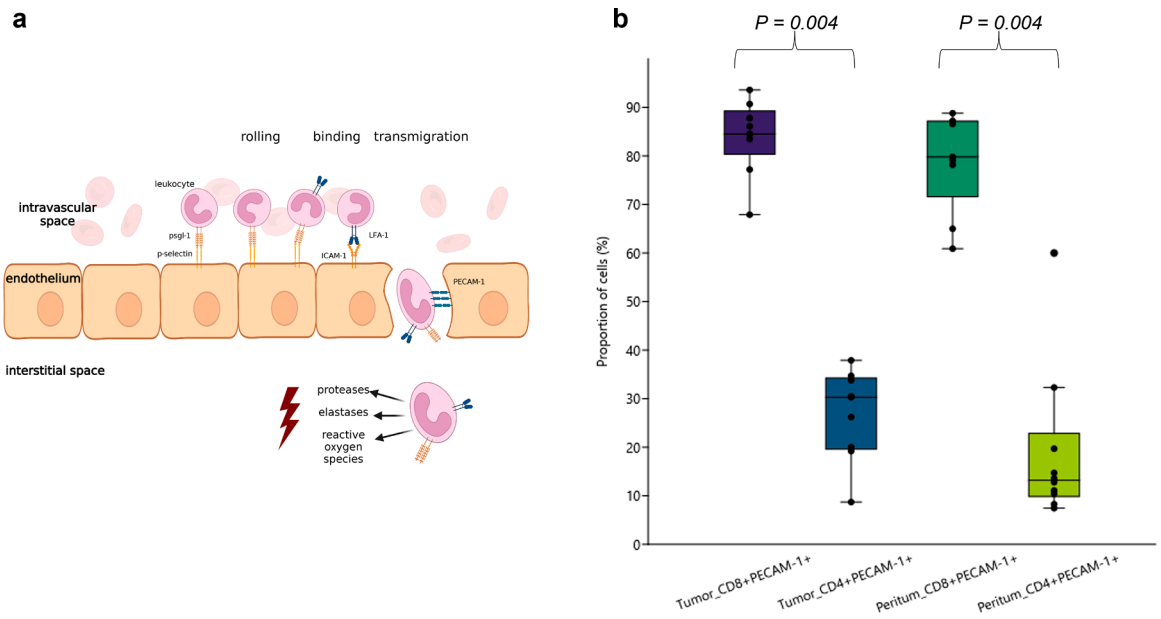

Fig. 3. Figure 2. PECAM-1 expression in $CD8^+$ and $CD4^+$ T cells. A: graphical depiction of PECAM-1-mediated transendothelial migration of T cells. B: boxplots of relative abundance of CD8+PECAM-1+ and CD4+PECAM-1+ in the tumoral and peritumoral compartments. The percentile range was set at 25 %, 50 %, and 75 %. The whisker range was chosen to be between minimal and maximal measured values with outliners.

Using flow cytometry, we assessed the distribution of FasL, a key antitumor cytotoxic molecule, and CD107a, a general marker of T cell degranulation in the $CD4^+$ and $CD8^+$ T cell subpopulations [30,31]. In tumor tissues, $CD4^+$ T cells expressed significantly higher levels of CD107a than $CD8^+$ T cells ($P = 0.04$), whereas $CD8^+$ T cells predominantly expressed FasL, and their proportion was significantly higher in the tumor tissue than that of FasL-positive $CD4^+$ T cells ($P = 0.008$). This distribution was more evident in the peritumoral tissue ($P_{CD107a} = 0.007$; $P_{FasL} = 0.002$), suggesting that within the TME, $CD8^+$ T cells mainly exploit FasL, while $CD4^+$ T cells exploit CD107a (Fig. 4a-b). FasL expression was negatively correlated with CD107a expression in tumor-infiltrating $CD8^+$ T cells, implying that the prevailing type of cytotoxic response limited the other one (Fig. 4c). With over 90 % of FasL-positive $CD8^+$ T cells in the tumor tissue, our findings indicate that FasL is the major molecule responsible for antitumor cytotoxicity. Our discovery that, in RCC tumors, $CD8^+$ T cells primarily employ FasL, while $CD4^+$ T cells depend on degranulation through CD107a, has prompted us to investigate the correlation between these cytotoxic phenotypes and survival outcomes. Thus, we have examined the relationship between tumoral and peritumoral CD4/CD8 cells positive for CD107a/FasL, in association with patient mortality in a subset of patients. On average, patients experienced a 20-month survival period with a medium follow-up 62 months. Neither tumoral nor peritumoral $CD4^+$ and $CD8^+$ T cells expressing FasL showed any correlation with patient survival. However, our data demonstrated a statistically significant negative correlation between the presence of $CD4^+CD107^+$ pTILs and patient mortality, as shown in **Supplementary Figure 2.**

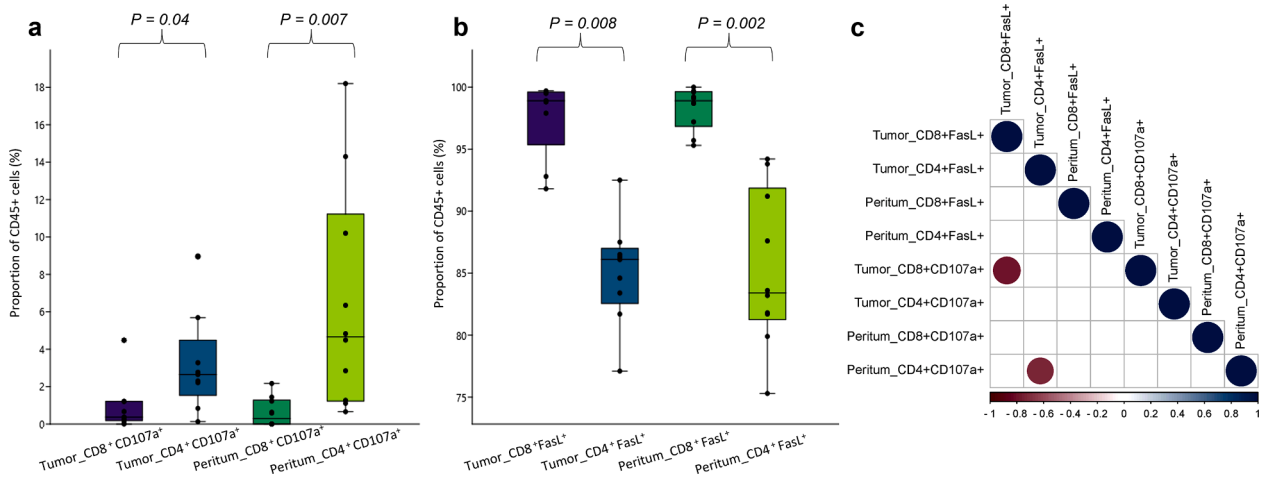

Fig. 4. Cytotoxic capacity of T cells in tumoral and peritumoral compartments. A: boxplots of relative abundance of $CD8^+CD107a^+$ T cells and $CD4^+CD107a^+$ T cells. B: boxplots of relative abundance of $CD8^+FasL^+$ and $CD4^+$ $FasL^+$T cells. The percentile range was set at 25 %, 50 %, and 75 %. The whisker range was chosen to be between minimal and maximal measured values with outliners. C: Association of the tumoral and peritumoral production of CD107a and FasL. The coefficient of correlation of variables is presented by a coloring scheme from red (negative correlation) to blue (positive correlation), whereas white represents an absence of correlation. FasL: fas ligand; peritum: peritumoral.

TILs produce higher levels of cytokines compared to pTILs

After assessing the cytotoxic ability of peritumoral and intra-tumoral T cells, we characterized their secretory profile. Using the Luminex assay, we investigated cytokine production in tumor, peritumoral, healthy renal tissues, and peripheral blood of RCC patients. Age significantly influenced basal production of CXCL10 ($P < 0.001$) and FasL ($P = 0.007$) in non-stimulated peritumoral tissues. Selected clinicopathological variables and their correlations with basal cytokine production are shown in **Supplementary Figure 3.**

Most importantly, the tumor compartment had the highest basal levels of cytokines **(Supplementary Table 1)** in all patients, indicating that TILs secrete more inflammatory cytokines, and are thus more active than naïve pTILs.

TILs were shown to be the primary source of cytotoxic markers IFN-γ, granzyme B, and FAS ligand

Next, we analyzed the production of four distinctive cytotoxic cytokines (TRAIL, IFN-γ, granzyme B, and FasL) in the tumor, peritumoral tissue, healthy renal tissue, and PBMCs. These compartments differed notably in their production of TRAIL ($P = 0.004$). The tumor tissue had the highest TRAIL levels as compared to other tissue compartments. The pTILs also produced relatively high levels of TRAIL, while PBMCs had the lowest TRAIL levels (Fig. 5a). IFN-γ levels were highest in the tumor tissue, followed by those in the peritumoral tissue (Fig. 5b). In the pTILs, IFN-γ levels correlated positively with granzyme B levels (both $P = 0.0004$). This phenomenon was also observed in the adjacent healthy renal tissue. Contrarily, IFN-γ produced by PBMCs negatively correlated with the granzyme B produced by pTILs ($P = 0.003$) **(Supplementary Figure 4).**

The basal production of granzyme B was relatively low in the peritumoral tissue (14.1 ± 7.6 pg/ml), adjacent healthy renal tissue (5.8 ± 2.6 pg/ml), and the PBMC compartment (Fig. 5c). In addition, in the peritumoral tissue, high basal levels of granzyme B were significantly associated with elevated levels of CXCL9 ($P = 0.0004$) **(Supplementary Figure 4).**

The tumor tissue had the highest levels of FasL in the non-stimulated cell suspensions (Fig. 5d). In the peritumoral tissue, FasL expression correlated with granzyme B levels ($P = 0.006$), whereas in the healthy renal tissues, it was associated with an increase in both IFN-γ and granzyme B levels **(Supplementary Figure 4).**

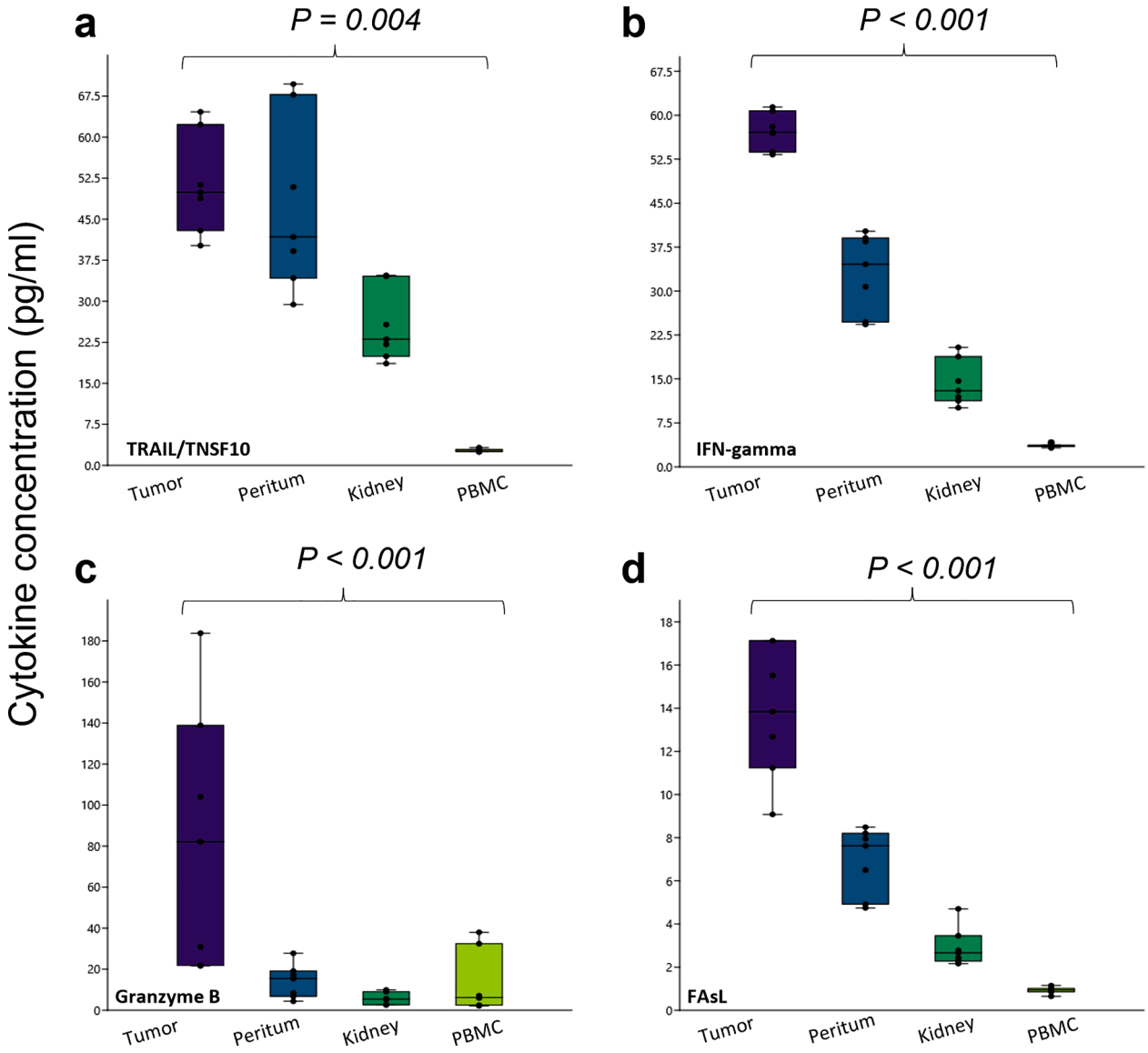

Fig. 5. Cytokine production by immune cells infiltrating different tissue compartments (tumor, peritumor, healthy renal tissue, peripheral blood). a: TRAIL/TNSF10; b: IFN-gamma; c: granzyme B; d: FasL. FasL: fas ligand; IFN-gamma: interferon gamma; Kidney: healthy renal tissue; peritum: peritumor; PMBC: peripheral blood.

TRAIL and FAS receptors are more prevalent in tissue compartments than in peripheral blood of rcc patients

Considering the high production of TRAIL and FasL, our aim was to explore the corresponding receptor expression for these ligands. Our analyses in a subgroup of patients, along with two additional healthy controls, revealed that the expression of TRAIL receptors within the peripheral blood was particularly low in both patient and control groups (Fig. 6a). However, within tissue compartments, this expression exceeded 30 %. Furthermore, when considering interindividual variability, it became evident that some patients exhibited TRAIL receptor expression in over 80 % of non-leukocytic cells.

The expression of the Fas receptor was observed in both immune cells and non-immune cells across different compartments. In $CD3^+$ T cells, the expression of Fas receptor was higher than the expression of TRAIL receptor. As shown in Fig. 6b, $FasR^+CD4$ and $CD8^+$ T cells were more abundant in the tissue compartments of RCC patients than in the peripheral blood of healthy controls. This finding aligns with prior studies that underscore the crucial role of the Fas-Fas ligand axis in the tumor microenvironment (TME) [32,33].

Peritumoral $CD4^+$ and $CD8^+$ T cells are the major players in the PD-1 and PD-L1 signaling pathway

Dysregulated tumor control is a contributing factor to TIL exhaustion. Given the relatively high basal production of cytotoxic cytokines by TILs in our study, our objective was to investigate their involvement in the checkpoint signaling through the PD-1 and PD-L1 pathway. PD-L1 is the most widely adopted tissue-based biomarker that has become a predictor of patient survival and response to PD1/PD-L1 monotherapy [34–36].

Hence, we assessed the expression of PD-L1 in $CD4^+$ and $CD8^+$ T cells, as well as in the non-leukocytic fraction, across four distinct compartments: peripheral blood, adjacent healthy renal tissue, peritumoral tissue, and tumor tissue. Additionally, we included two non-oncologic control patients and evaluated PD-L1 expression in their peripheral blood.

As shown in Fig. 7a, we observed significantly higher PD-L1 surface expression in tissue compartments compared to the peripheral blood compartment. Upon closer examination of the tissue compartments, it became apparent that $CD4^+$ and $CD8^+$ pTILs exhibited the most pronounced involvement in the PD-1/PD-L1 pathway (Fig. 7b). Interestingly, PD-L1 expression in the non-leukocyte fraction of the tumor tissue was relatively lower than in their leukocytic counterparts, suggesting that the immune exhaustion may be result of a chronic overstimulation rather than being primarily caused by the effects of PD-L1.

Peripheral blood T cells elicit stronger responses to stimulation than TILs and pTILs

The highest levels of cytotoxic cytokines were produced by TILs in the tumor compartment, presumably because of continuous antigen exposure. We then wondered if it could further enhance this antitumor response and cytotoxic cytokine secretion by directly stimulating T cells from the different compartments (tumor, peritumoral tissue, healthy kidney, and peripheral blood).

T cells isolated from the tumor tissues activated by superparamagnetic polymer beads increased IFN-γ and PECAM-1 production, while in the peritumoral tissue and healthy renal tissue, PECAM-1 and FasL expression was increased. In the PBMCs, the levels of most of the tested cytokines increased in response to T cell stimulation because this compartment contains a high proportion of naïve, unstimulated T cells (**Supplementary Table 1**).

The most profound responses to stimulation were reflected in IFN-γ and CXCL-10 levels (**Supplementary Table 1**). Post stimulation, the peripheral blood compartment showed the most significant increase in IFN-γ ($P = 0.016$) and FasL ($P = 0.003$) levels. These findings suggest that tumor and peritumoral T cells may only marginally respond to further activation signals.

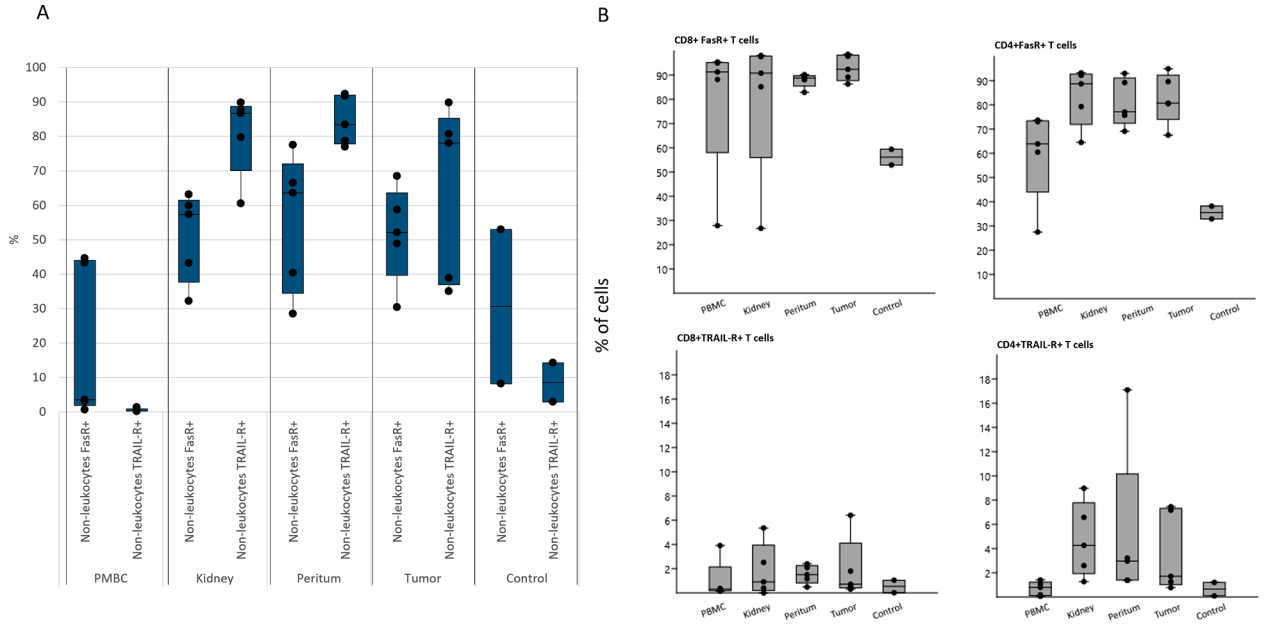

Fig. 6. The expression of Fas and TRAIL receptor in leukocyte and non-leukocyte cells A: boxplots of relative abundance of FasR/TRAIL-R positive non-leukocyte cells infiltrating different tissue compartments (tumor, peritumoral tissue, healthy renal tissue, peripheral blood, control – peripheral blood of healthy donors). B: boxplots of relative abundance of FasR/TRAIL-R positive CD4/CD8 T-cells infiltrating different tissue compartments (tumor, peritumoral tissue, healthy renal tissue, peripheral blood, control – peripheral blood of healthy donors). The percentile range was set at 25 %, 50 % and 75 %. The whisker range was chosen to be between minimal and maximal measured value. Kidney: healthy renal tissue; peritum: peritumoral tissue; PBMC: peripheral blood mononuclear cells; control: healthy donor PBMCs.

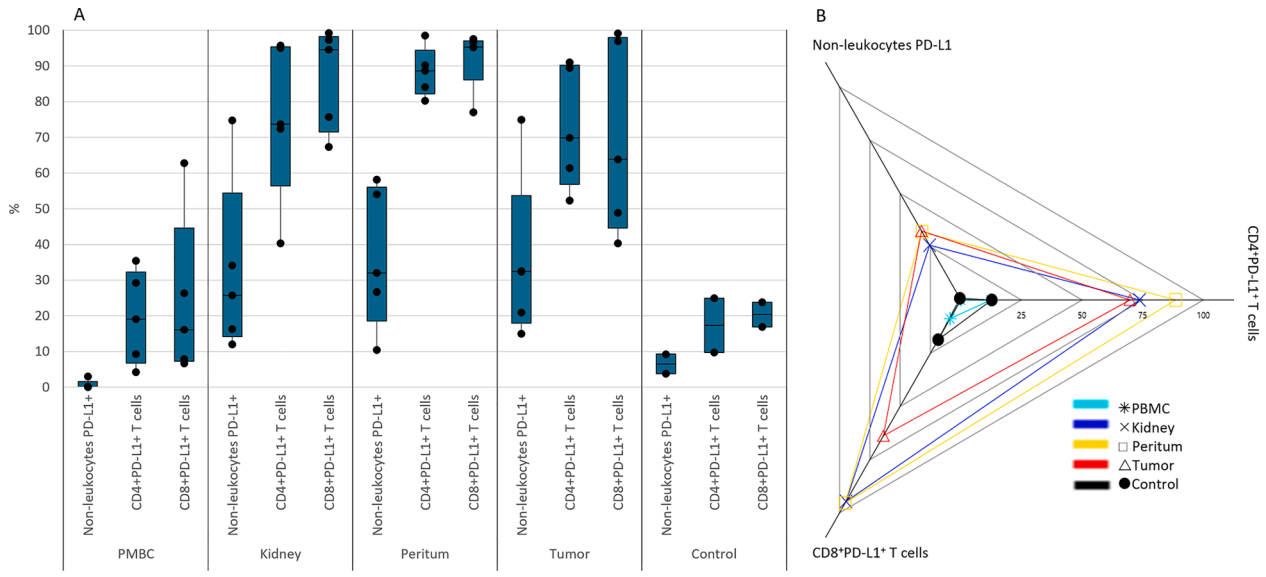

Fig. 7. Categorical analysis of PD-L1 expression in distinct cell subpopulations within tissue compartments of RCC patients and in the peripheral blood of healthy donors. A: boxplots of relative abundance of PD-L1 positive cells infiltrating different tissue compartments (tumor, peritumoral tissue, healthy renal tissue, peripheral blood, control - peripheral blood of healthy donors). The percentile range was set at 25 %, 50 % and 75 %. The whisker range was chosen to be between minimal and maximal measured value. B: radar chart presenting the median percentage content of PD-L1 positive cells in different compartments. Kidney: healthy renal tissue; peritum: peritumoral tissue; PBMC: peripheral blood mononuclear cells; control: healthy donor PBMCs.

Increased CXCL-10 levels following stimulation are related to high FAS ligand and IFN-γ levels

The chemokines CXCL-9 and CXCL-10 allow T cells to migrate efficiently into the TME [37]. In response to stimulation, elevation in CXCL-10 level was the highest in the peripheral blood ($P = 0.015$), tumor tissue ($P = 0.014$), and healthy renal tissue ($P = 0.049$) (Fig. 8a).

Furthermore, in RCC tumors, elevated levels of CXCL-10 post stimulation correlated with an increase in FasL ($P = 0.0004$) and IFN-γ ($P = 0.007$) levels, indicating a cooperative role of these cytokines (Fig. 8b). In contrast, the pTILs produced more granzyme B ($P = 0.02$) and less TRAIL ($P = 0.01$) in the presence of CXCL-10.

CXCL-9 chemokine was unrelated to clinicopathological variables or other cytokines and tissue compartments. However, in the peritumoral compartment (non-stimulated cells), IFN-γ production was positively associated with granzyme B ($P = 0.0004$) (data not shown) and CXCL-9 ($P = 0.0004$) production (Fig. 8c).

Discussion

Up to 30 % of patients with RCC are diagnosed at the metastatic phase [3,9]. While immunotherapy is promising, a substantial proportion of patients is resistant [38]. Previously, we have shown that RCC's peritumoral tissue constitutes a reservoir of cytotoxic/migratory NK cells and T cells[16]. In the current study, we attempted to characterize T cell subpopulations infiltrating distinct tissue compartments in patients with RCC.

CAFs are known to alter the TME composition and affect immune cell trafficking [23]. Yet, we observed only a small proportion of CAFs, suggesting their limited impact on T cells. On the other hand, we showed a correlation between PECAM-1 expression in $CD8^+$ T cells and CAFs suggesting a role of CAFs in modulation of transendothelial migration [16,23]. We also observed a significantly higher expression of PECAM-1 in $CD8^+$ T cells as compared to $CD4^+$ T cells. Interestingly, lower PECAM-1 levels were observed in pTILs as compared to TILs. Since PECAM-1 expression has been implicated in various T cell processes, we hypothesized that the downregulation of PECAM-1 in the peritumoral compartment might play a role in protection of $CD8^+$ T cells from excessive activation and damage in inflamed tumor tissue [28,29,39]. On the other hand, it may retain $CD8^+$ T cells in the peritumoral area to preserve their active state before infiltrating the tumor [29,39].

For the first time in RCC tumors, we show that the $CD8^+$T cells predominantly use FasL, while $CD4^+$ T cells rely on degranulation via CD107a. Additionally, a statistically significant adverse correlation between patient survival and the presence of $CD4^+CD107^+$ pTILs was observed. Given that various studies have indicated that $CD4^+$ T cells have a significant role in antitumor immunity, we presume that the expression of CD107a might represent a potential biomarker, and further evaluation of its functions in intratumoral $CD4^+$ T cells is needed [40–42].

Although TILs and pTILS are characterized by unique surface markers, it remains unclear whether the differences in marker expression correspond to phenotypically distinct T cells with modified function and spatially distinct cytokine secretion profiles. Thus, we examined the extent to which these differences could impact antitumor immunity.

TRAIL levels showed the most profound differences between compartments, with the highest levels in the tumor tissue. FasL and IFN-γ levels were also the highest in the tumor tissue, and positively correlated with elevated granzyme B levels, suggesting the coordinated action of these cytotoxic cytokines. We also stimulated the cells and, to our surprise, T cell stimulation increased IFN-γ and PECAM-1 expression in TILs, and PECAM-1 and FasL expression in the pTILs and healthy tissue-infiltrating lymphocytes. PBMCs showed an increase in the levels of most cytokines tested following T cell-specific stimulation. The IFN-γ and CXCL-10 (highest response rate) levels reflected the most significant responses to stimulation.

The engagement with the PD-1/PD-L1 pathway was more evident in $CD4^+$ and $CD8^+$ pTILs as opposed to TILs. Moreover, PD-L1 expression in the non-leukocyte fraction of the tumor tissue was relatively lower than in their leukocytic counterparts indicating that immune exhaustion might stem from chronic overstimulation rather than being primarily attributed to the effects of PD-L1.

This study has several limitations. A major limitation of this study is the small sample size of enrolled patients. Furthermore, we were only able to observe and analyze the samples collected at a single time point, thus, we could not track the changes that may occur in the TME over time. Another important limitation is that, while we successfully demonstrated the *in vitro* production of cytotoxic cytokines and

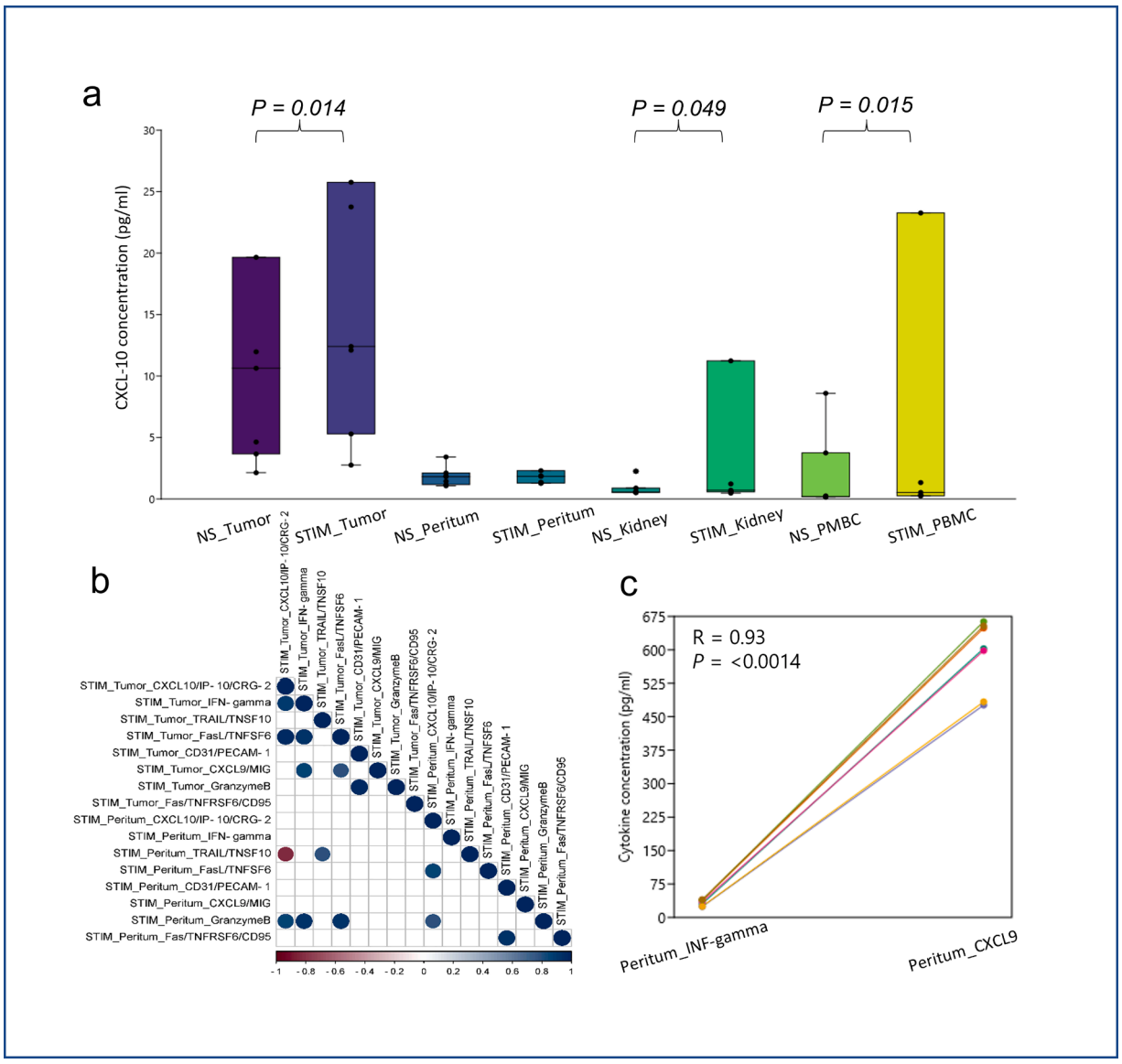

Fig. 8. Chemokine production by stimulated/ non-stimulated immune cells in different tissue compartments (tumor, peritumor, healthy renal tissue, peripheral blood). A: CXCL-10 production in stimulated/ non-stimulated T cells B: Association of the chemokines' and cytokines' production. The coefficient of correlation of variables is presented by a coloring scheme from red (negative correlation) to blue (positive correlation), whereas white represents an absence of correlation.C: correlation between IFN-gamma and CXCL9 production in peritumoral tissue. FasL: fas ligand; IFN-gamma: interferon gamma; Kidney: healthy renal tissue; peritum: peritumor; PMBC: peripheral blood.

elucidated various mechanisms through which TILs and pTILs may participate in tumor elimination, we did not directly exhibit the elimination of tumor cells in controlled laboratory settings. This direct demonstration would better illustrate the actual tumor-specific killing capacity. Further investigation in a larger and ideally prospective study is necessary to confirm the observed associations with clinical outcomes and treatment response.

Conclusion

In conclusion, tumor and peritumoral T cells may only marginally respond to further activation signals. The pool of circulating peripheral T cells retains the capacity to respond to stimulatory signals, suggesting that strategies enhancing T cell trafficking into tumor might be potentially useful in RCC.

CRediT authorship contribution statement

Martina Borcinova: Writing – review & editing, Visualization, Validation, Software, Formal analysis, Data curation, Conceptualization. **Robin Bartolini:** Writing – review & editing, Writing – original draft, Validation, Methodology, Investigation, Conceptualization. **Lily Koumbas Foley:** Visualization, Investigation, Conceptualization. **Vojtech Novak:** Writing – review & editing, Methodology, Investigation, Data curation. **Pavla Taborska:** Writing – review & editing, Validation, Conceptualization. **Dmitry Stakheev:** Writing – review & editing, Conceptualization. **Michal Rataj:** Writing – review & editing, Methodology, Formal analysis, Data curation. **Daniel Smrz:** Writing – review & editing, Supervision, Resources. **Martina Fialova:** Writing – review & editing, Formal analysis, Data curation. **Jaromir Hacek:** Methodology, Investigation, Writing – review & editing. **Martin Komarc:** Data curation, Validation, Writing – review & editing. **Stepan Vesely:** Writing – review & editing, Supervision, Conceptualization. **Marek Babjuk:** Writing – review & editing, Supervision, Formal analysis. **Ilja Striz:**

Writing – review & editing, Validation, Supervision. **Jirina Bartunkova:** Writing – review & editing, Supervision. **Tomas Buchler:** Writing – review & editing, Validation, Supervision, Formal analysis. **Zuzana Ozaniak Strizova:** Conceptualization, Methodology, Formal analysis, Investigation, Writing – original draft, Supervision, Funding acquisition.

Declaration of competing interest

The authors declare no conflict of interest. Jirina Bartunkova reports a relationship with Sotio Biotech as that includes: employment.

Acknowledgement

The authors would like to express their sincere gratitude to the technical staff and patients who made this study possible. Their support and participation were invaluable to the successful completion of this research.

Declaration of generative AI in scientific writing

During the preparation of this work, the English language has been reviewed and improved using an AI language model, specifically ChatGPT. This tool was used solely for linguistic assistance and did not contribute to the scientific content, analysis, or interpretation of the study. After using this tool, the authors reviewed and edited the content as needed and take full responsibility for the content of the publication.

Funding

Research was supported by funding from the Ministry of Health, Czech Republic - projects AZV NU23J-08–00031; NU22–03–00300 and NU23–08–00071.

Supplementary materials

Supplementary material associated with this article can be found, in the online version, at doi:10.1016/j.tranon.2024.101891.

References

[1] J.J. Hsieh, M.P. Purdue, S. Signoretti, C. Swanton, L. Albiges, M. Schmidinger, et al., Renal cell carcinoma, Nat. Rev. Disease Primers 3 (2017) 17009.
[2] L. Albiges, V. Molinie, B. Escudier, Non-clear cell renal cell carcinoma: does the mammalian target of rapamycin represent a rational therapeutic target? Oncologist 17 (8) (2012) 1051–1062.
[3] R.J. Motzer, B. Escudier, D.F. McDermott, S. George, H.J. Hammers, S. Srinivas, et al., Nivolumab versus everolimus in advanced renal-cell carcinoma, New Engl. J. Med 373 (19) (2015) 1803–1813.
[4] J. Tran, M.C. Ornstein, Clinical review on the management of metastatic renal cell carcinoma, JCO. Oncol. Practice. 18 (3) (2022) 187–196.
[5] B.I. Rini, E.R. Plimack, V. Stus, R. Gafanov, R. Hawkins, D. Nosov, et al., Pembrolizumab plus axitinib versus sunitinib for advanced renal-cell carcinoma, N. Engl. J. Med 380 (12) (2019) 1116–1127.
[6] R.J. Motzer, K. Penkov, J. Haanen, B. Rini, L. Albiges, M.T. Campbell, et al., Avelumab plus axitinib versus sunitinib for advanced renal-cell carcinoma, N. Engl. J. Med 380 (12) (2019) 1103–1115.
[7] R.J. Motzer, N.M. Tannir, D.F. McDermott, O. Arén Frontera, B. Melichar, T. K. Choueiri, et al., Nivolumab plus ipilimumab versus sunitinib in advanced renal-cell carcinoma, N. Engl. J. Med 378 (14) (2018) 1277–1290.
[8] T.K. Choueiri, T. Powles, M. Burotto, B. Escudier, M.T. Bourlon, B. Zurawski, et al., Nivolumab plus cabozantinib versus sunitinib for advanced renal-cell carcinoma, N. Engl. J. Med 384 (9) (2021) 829–841.
[9] J. Tran, M.C. Ornstein, Clinical review on the management of metastatic renal cell carcinoma, JCO. Oncol. Pract 18 (3) (2022) 187–196.
[10] S. Bagchi, R. Yuan, E.G. Engleman, Immune Checkpoint Inhibitors for the Treatment of Cancer: clinical Impact and Mechanisms of Response and Resistance, Annual Rev. Pathol.:. Mechan. Disease 16 (1) (2021) 223–249.
[11] M.Y. Chen, Y.C. Zeng, Pseudoprogression in lung cancer patients treated with immunotherapy, Crit. Rev. Oncol. Hematol. 169 (2022) 103531.
[12] B.A. Taleb, Tumour flare reaction in cancer treatments: a comprehensive literature review, Antican. Drugs 30 (9) (2019) 953–958.
[13] D.J. McGrail, P.G. Pilié, N.U. Rashid, L. Voorwerk, M. Slagter, M. Kok, et al., High tumor mutation burden fails to predict immune checkpoint blockade response across all cancer types, Annal. Oncol 32 (5) (2021) 661–672.
[14] W.H. Fridman, J. Galon, F. Pagès, E. Tartour, C. Sautès-Fridman, G. Kroemer, Prognostic and predictive impact of intra- and peritumoral immune infiltrates, Cancer Res 71 (17) (2011) 5601–5605.
[15] S.W. Sorbye, T.K. Kilvaer, A. Valkov, T. Donnem, E. Smeland, K. Al-Shibli, et al., Prognostic impact of peritumoral lymphocyte infiltration in soft tissue sarcomas, BMC. Clin. Pathol 12 (2012) 5.
[16] Z. Strizova, P. Taborska, D. Stakheev, S. Partlová, K. Havlova, S. Vesely, et al., NK and T cells with a cytotoxic/migratory phenotype accumulate in peritumoral tissue of patients with clear cell renal carcinoma, Urol. Oncol 37 (7) (2019) 503–509.
[17] F. Sabbatino, G. Scognamiglio, L. Liguori, A. Marra, A.M. Anniciello, G. Polcaro, et al., Peritumoral immune infiltrate as a prognostic biomarker in thin melanoma, Front. Immunol 11 (2020) 561390.
[18] C. Keun Park, S. Kyum Kim, Clinicopathological significance of intratumoral and peritumoral lymphocytes and lymphocyte score based on the histologic subtypes of cutaneous melanoma, Oncotarget 8 (9) (2017).
[19] W.H. Fridman, J. Galon, F. Pagès, E. Tartour, C. Sautès-Fridman, G. Kroemer, Prognostic and predictive impact of intra- and peritumoral immune infiltrates, Cancer Res. 71 (17) (2011) 5601–5605.
[20] O. Brück, M.H. Lee, R. Turkki, I. Uski, P. Penttilä, L. Paavolainen, et al., Spatial immunoprofiling of the intratumoral and peritumoral tissue of renal cell carcinoma patients, Modern. Pathol 34 (12) (2021) 2229–2241.
[21] D.A. Braun, Y. Hou, Z. Bakouny, M. Ficial, M. Sant' Angelo, J. Forman, et al., Interplay of somatic alterations and immune infiltration modulates response to PD-1 blockade in advanced clear cell renal cell carcinoma, Nat. Med. 26 (6) (2020) 909–918.
[22] L. Gorchs, C. Fernández Moro, P. Bankhead, K.P. Kern, I. Sadeak, Q. Meng, et al., Human pancreatic carcinoma-associated fibroblasts promote expression of co-inhibitory markers on CD4(+) and CD8(+) T-cells, Front. Immunol 10 (2019) 847.
[23] T.J. Harryvan, E.M.E. Verdegaal, J.C.H. Hardwick, L. Hawinkels, S.H. van der Burg, Targeting of the cancer-associated fibroblast-T-cell axis in solid malignancies, J. Clin. Med 8 (11) (2019).
[24] T. Kinoshita, G. Ishii, N. Hiraoka, S. Hirayama, C. Yamauchi, K. Aokage, et al., Forkhead box P3 regulatory T cells coexisting with cancer associated fibroblasts are correlated with a poor outcome in lung adenocarcinoma, Cancer. Sci 104 (4) (2013) 409–415.
[25] H. Salmon, K. Franciszkiewicz, D. Damotte, M.C. Dieu-Nosjean, P. Validire, A. Trautmann, et al., Matrix architecture defines the preferential localization and migration of T cells into the stroma of human lung tumors, J. Clin. Invest 122 (3) (2012) 899–910.
[26] E. Sahai, I. Astsaturov, E. Cukierman, D.G. DeNardo, M. Egeblad, R.M. Evans, et al., A framework for advancing our understanding of cancer-associated fibroblasts, Nat. Rev. Cancer 20 (3) (2020) 174–186.
[27] T. Liu, C. Han, S. Wang, P. Fang, Z. Ma, L. Xu, et al., Cancer-associated fibroblasts: an emerging target of anti-cancer immunotherapy, J. Hematol. Oncol 12 (1) (2019) 86.
[28] D.K. Newman, G. Fu, T. Adams, W. Cui, V. Arumugam, T. Bluemn, et al., The adhesion molecule PECAM-1 enhances the TGF-β–mediated inhibition of T cell function, Sci. Signal 9 (418) (2016) ra27–rara.
[29] E.A. Ross, R.E. Coughlan, A. Flores-Langarica, S. Bobat, J.L. Marshall, K. Hussain, et al., CD31 is required on CD4+ T cells to promote T cell survival during salmonella infection, The. J. Immunol 187 (4) (2011) 1553–1565.
[30] J. O'Connell, Fas ligand and the fate of antitumour cytotoxic T lymphocytes, Immunology 105 (3) (2002) 263–266.
[31] G. Alter, J.M. Malenfant, M. Altfeld, CD107a as a functional marker for the identification of natural killer cell activity, J. Immunol. Methods 294 (1–2) (2004) 15–22.
[32] J. Zhu, P.F. Petit, .BJ Van den Eynde, Apoptosis of tumor-infiltrating T lymphocytes: a new immune checkpoint mechanism, Cancer Immunol., Immunother.: CII 68 (5) (2019) 835–847.
[33] M. Kuchar, Z. Strizova, M. Votava, J. Plzak, The relevance of Fas/Fas ligand axis in the tumor microenvironment of salivary gland adenoid cystic carcinoma, Oral. Oncol 97 (2019) 135–136.
[34] M.B. Saad, L. Hong, M. Aminu, N.I. Vokes, P. Chen, M. Salehjahromi, et al., Predicting benefit from immune checkpoint inhibitors in patients with non-small-cell lung cancer by CT-based ensemble deep learning: a retrospective study, Lancet Digital Heal 5 (7) (2023) e404–ee20.
[35] X.J. Chen, S.Q. Yuan, J.L. Duan, Y.M. Chen, S. Chen, Y. Wang, et al., The value of PD-L1 expression in predicting the efficacy of anti-PD-1 or anti-PD-L1 therapy in patients with cancer: a systematic review and meta-analysis, Dis. Markers 2020 (2020) 6717912.
[36] M. Yi, D. Jiao, H. Xu, Q. Liu, W. Zhao, X. Han, et al., Biomarkers for predicting efficacy of PD-1/PD-L1 inhibitors, Mol. Cancer 17 (1) (2018) 129.
[37] H. Bronger, J. Singer, C. Windmüller, U. Reuning, D. Zech, C. Delbridge, et al., CXCL9 and CXCL10 predict survival and are regulated by cyclooxygenase inhibition in advanced serous ovarian cancer, Br. J. Cancer 115 (5) (2016) 553–563.
[38] N. Singla, V. Margulis, Locally advanced kidney cancer: a new space for immunotherapy? Europ. Urol. Oncol 5 (1) (2022) 118–119.
[39] L. Ma, K.C. Cheung, M. Kishore, S. Nourshargh, C. Mauro, F.M. Marelli-Berg, CD31 exhibits multiple roles in regulating T lymphocyte trafficking in vivo, J. Immunol. (Baltimore,. Md:. 1950) 189 (8) (2012) 4104–4111.

[40] D.S. Kravtsov, A.K. Erbe, P.M. Sondel, A.L. Rakhmilevich, Roles of CD4+ T cells as mediators of antitumor immunity, Front. Immunol 13 (2022).
[41] L. Leclair, S. Depil, [CD4(+) T Lymphocytes: major players in antitumor immune response], Med. Sci. (Paris) 37 (6–7) (2021) 671–673.
[42] T. Li, B. Wu, T. Yang, L. Zhang, K Jin, The outstanding antitumor capacity of CD4+ T helper lymphocytes, Biochimica. et Biophysica. Acta (BBA). -. Rev. Cancer 1874 (2) (2020) 188439.